Geometric error compensation through position feedback modification and comparison of correction strategies in 3- axis machine-tool

Flore Guevel[a], Fabien Viprey[a], Charly Euzenat[a], Guillaume Fromentin[a] and Ugo Masciantonio[b]

[a]Arts et Métiers Institute of Technology, LABOMAP, Rue Porte de Paris, Cluny, F-71250, France
[b]CETIM, 52 avenue Félix Louat, Senlis, F-60300, France

ARTICLE INFO

Keywords:
Error compensation
Real-time software
Geometric error
3-axis machine-tool
High-accuracy machining

ABSTRACT

In machine-tools, geometrical defects are unavoidable. They can greatly affect the dimensional accuracy of the final workpiece if not corrected. Software compensation strategies are less expensive than mechanical adjustments and they provide great improvement in volumetric accuracy. In this study, different compensation methods are compared in a 3-axis milling applications: Numerical Controller (NC) internal compensation tables, modification of the programmed tool-path (G-code) and modification of position feedback signals. The latter is the main purpose of this work, because it shows great potential and is not linked to one particular type of NC. It communicates with a custom software application that processes the position data and generates corrected signals according to a geometric model based on the rigid body assumption. The NC is then induced to perform volumetric error correction based on its default programming. The compensation methods are compared based on their ability to bring out or correct imposed geometric errors. The highlighted solution shows performances comparable to the G-code modification by correcting more than 96% of the imposed geometric errors without affecting the numerical chain from the program generation to its execution on the machine. It is also independent of the NC or the motors control cards.

1. Introduction

The dimensional accuracy of a machined part can be influenced by numerous factors. On the one hand, the machining strategy, workpiece clamping, cutting parameters and tool wear play a key role in the final result. On the other hand, the machine-tool itself and its environment represent other significant error sources by introducing a deviation of the tool in the workpiece coordinate system in relation to the CAM instructions. In their review articles, Gao et al. [1] and Schwenke et al. [2] classify these machine-related error sources into geometric inaccuracies, thermally-, static load- and dynamically-induced errors. According to Ramesh [3] and Andolfatto [4], quasi-static errors are mainly responsible for the volumetric error in the machine workspace, accounting for 70-90% of the total machining inaccuracy. The more axes the machine has, the more complex the modelling, identification and compensation of these errors are. They can be identified through direct methods such as the use of a laser interferometer like Ibaraki in [5], or indirect methods such as ball-bar measurements [6], the use of calibrated artefacts like in the SAMBA methodology proposed by Alami Mchichi and Mayer [7], or the machining of test pieces [8]. Finally, once the machine behaviour and performance is described by an identified model, software compensation strategies can be implemented [9].

This research work emphasizes on geometric error software compensation methodologies in machine-tools. The aim of software compensation is to correct the positioning of the tool after evaluating the volumetric error at each point of the tool-path. Several methods are possible. The re-computation of the tool-path via a geometric error model and the modification of NC code accordingly is straightforward. It does not require specific hardware and is often used by researchers to validate a machine modelling or a compensation algorithm, which are complex for 5-axis machines [10–12]. However, it is not the best industrial strategy because each program is linked to a part and a machine; the program is referenced to a specific origin point within each machine workspace. Furthermore, the G-code becomes less understandable for the machine operator. Some other compensation methods rely on the Numerical Controller (NC) and run in real-time. For instance, compensation tables can be filled with axis motion and link errors and these data are directly considered in the position control loop, although some NC have a limited number of compensation points and cannot perform effective multi-axis error compensation. Otherwise, when the NC is customizable enough, compensation algorithms can be implemented with the use of look-up tables. This is, for instance, the work of Esmaeili et al. [13] on a Siemens 840-D, or Lu et al. when they verify their identification and compensation of dominant errors via an open CNC system [14].

The last compensation method is the interception and modification of position feedback signals, which has the key advantage of being independent from the NC and the machining program. This method has been exposed by Ni [15] via the injection or removal of encoder pulses in the feedback of servo loops. Navya et al. propose in [16] an electronic circuit architecture allowing the insertion or subtraction of pulses in a TTL encoder signal. In the previous century, Donmez [17] presented The Real-Time Error Corrector, which is also based on the principle of

flore.guevel@ensam.eu (F. Guevel)
ORCID(s): 0000-0001-6298-8585 (F. Guevel)

modifying the number of pulses and presented results of thermal error compensation on the two axes of a turn. The compensation was calculated every 20 ms. In the same vein, they mention modifying the NC following error register, which would allow the axes to be positioned with a slight offset [18]. The encoder signal modification has also been tested by Postlethwaite et al. [19] on a 5-axis machine using specific encoder interface cards. On the other hand, Gurauskis et al. compensate for the thermal expansion of linear encoders via the correction of the measuring system output [20]. They program an FPGA to receive, recognize, compensate and generate the absolute position value in less than 26 µs. FPGAs represent the most recent and fastest solution for modifying encoder signals today [20, 21].

The aim of this study is to propose a detailed solution for the feedback loop signal modification on a 3-axis machine-tool first, before comparing different software-based compensation methods in a machining application. Their performances are analysed through the acquisition of compensated and uncompensated axis trajectory data, but also in machining applications, via the control of the main functional surfaces on a Coordinate Measuring Machine (CMM). The report begins with the introduction of basic geometric elements for a good understanding of the work carried out (section 2). Afterwards, the proposed compensation solution is explained in details (section 3). Subsequently, the machining of two types of parts is presented (section 4). The first workpiece was machined for the comparison of three compensation strategies. To do so, 3 motion errors were imposed along the X-axis of the machine-tool (section 5). Finally, the last machining experiment assessed the ability of the position signal modification solution to compensate the impact of a 21-geometric error model, imposed by a modified NC program (section 6).

2. Basic theory in geometric error compensation of a three-axis machine-tool

Forward and inverse geometric models of a 3-axis machine tool are accessible when the machine is seen as a robot with rigid bodies only. On the one hand, the positioning of the tool relative to the part is a 6-components vector $\mathbf{P} = [x\ y\ z\ i\ j\ k]$ with $(x\ y\ z)$ the coordinates of the tool center point (TCP), and $(i\ j\ k)$ the tool orientation vector decomposition along the workpiece frame axes, which is supposed to stay constant because no rotational movement is involved. On the other hand, the 3 prismatic joint coordinates are given as $\mathbf{Q} = [X\ Y\ Z]$ in the machine coordinate system (example in Figure 1). Ideal and non-ideal kinematics are analytically obtained via the use of Homogeneous Transformation Matrices (HTMs). The structure of the machine is shown in Figure 1. The workbench is supported by X-axis. On the tool-chain, the spindle is supported by Z-axis and Y-axis sequentially.

2.1. Geometric errors

As defined in the ISO 230-1:2012 standard [22], a prismatic joint counts six position-dependent errors, also called motion errors. For instance, for the X-axis, these errors are:

- $E_{YX}(X)$, the horizontal straightness error
- $E_{ZX}(X)$, the vertical straightness error
- $E_{XX}(X)$, the linear positioning error
- $E_{iX}(X), i \in \{A,\ B,\ C\}$, the roll, pitch and yaw errors respectively (for an horizontal axis)

The impact of linear geometric errors is exclusively unwanted translation of the TCP whereas angular errors induce a small deviation of the tool vector. Therefore, the TCP is also slightly moved because of a lever-arm effect. This tool-tip error cannot be fully compensated in a machine-tool without rotary axis. In addition, there are three squareness errors between the 3 axes that can be caused by an inaccurate assembly of the machine-tool. These are the position-independent geometric errors. Their impact is depicted in Figure 1. Consequently, the total amount of geometric errors for the studied machine is equal to 21, among which, 3 only are constants.

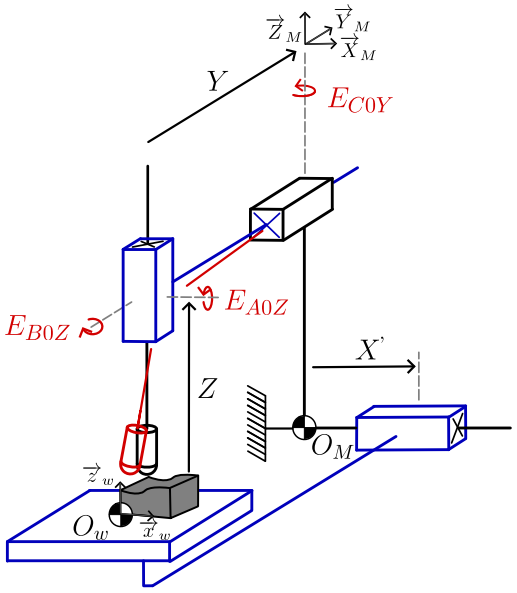

Figure 1: Kinematic structure of a 3-axis machine-tool, modelling the impact of three squareness errors (X being the reference axis)

In this study, no identification of the machine-tool's geometric errors was made. The proposed approach consists of imposing these errors. Their numerical values were chosen according to the literature [23]. Afterwards, they were generated by the compensation strategies instead of being corrected, as it is traditionally done. Therefore, the geometric accuracy of compensated machined parts is not closer to the CAD, but is the evidence of an artificial volumetric error.

2.2. Volumetric error

Four geometric models are required to perform modelling and correction of the impact of the previously introduced geometric errors :

- Ideal forward model: $\mathbf{P}_{\text{nominal}} = F_i(\mathbf{Q}_{\text{nominal}})$.
- Ideal inverse model: $\mathbf{Q}_{\text{nominal}} = I_i(\mathbf{P}_{\text{nominal}})$.
- Non-ideal forward model: $\mathbf{P}_{\text{actual}} = F_{ni}(\mathbf{Q}_{\text{actual}})$
- Non-ideal inverse model: $\mathbf{Q}_{\text{actual}} = I_{ni}(\mathbf{P}_{\text{actual}})$

The first two on the list are direct with the use of HTMs for prismatic joints. They are nominal models, I_i is the one implemented in the NC and the post-processor. Whereas the last two require more calculation with the introduction of error matrices [24]. They are supposed to represent the tool-tip deviation in the workpiece coordinate system. No further details are given on how these analytical models are obtained. However, the methodology of Ding et al. [25] to suppress high order terms in non-ideal geometric models was applied.

The volumetric error is a 6-component vector, depicted in Figure 2, and expressed in the workpiece reference frame as :

$$\mathbf{E}_v = \mathbf{P}_{\text{actual}} - \mathbf{P}_{\text{nominal}} = \begin{bmatrix} \delta x & \delta y & \delta z & \delta i & \delta j & \delta k \end{bmatrix} \quad (1)$$

It cannot precisely be measured in the machine workspace, especially during machining operations. This is why the geometric error model of the machine-tool needs to be identified in advance (or assumed, as in this work), before applying compensation methods.

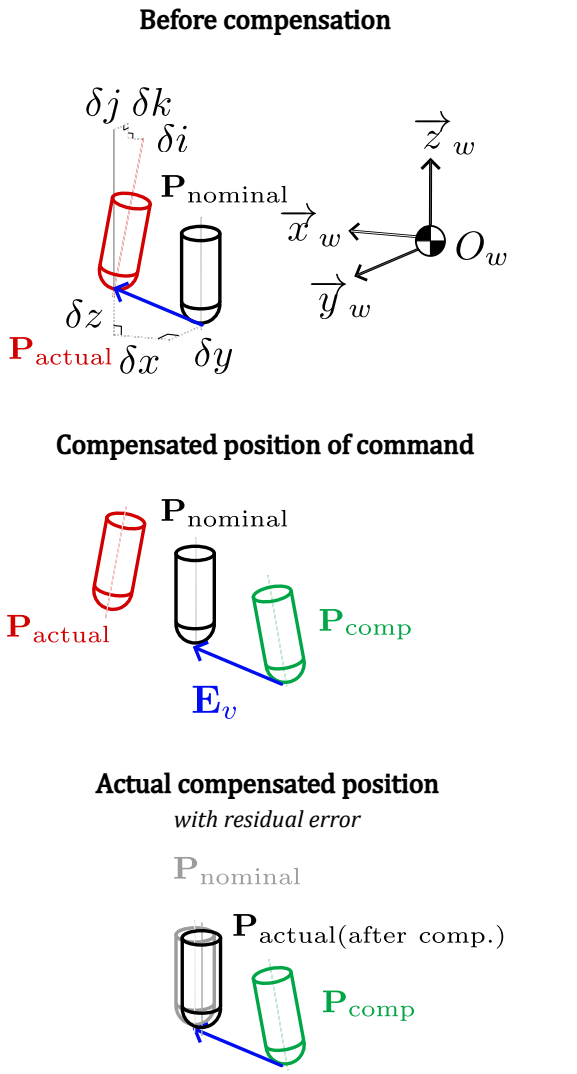

Figure 2: Example of a volumetric error definition and compensation

2.3. Software compensation

The principle of software compensation strategies is to modify the commanded position for any point of the tool-path. Indeed, as explained in Figure 2, the actual tool-tip is deviated from its desired positioning by the volumetric error vector. An assumption for small movements allows a linearisation of the error around the point at stake, and a new commanded position is generated for the tool with an anticipation of the estimated deviation. During the machining, the geometric errors (and other types of errors) change the tool direction from the programmed compensated tool-path, closer to its initially desired positioning. As explained in the introduction 1, there are several ways of modifying the tool-path of command. In this study, three strategies are compared.

2.3.1. Modified G-code

A simple way to correct an estimated volumetric error is to generate a new machining program. To do so, the nominal tool-path is discretised in smaller linear paths. This can introduce approximation errors and charges the program with multiple small displacements. Depending on the NC parameters, it can also lead to slowdowns. For each point of the trajectory $\mathbf{P}_{\text{nominal}}$, the nominal joints coordinates are estimated via the ideal inverse kinematics model (Equation 2).

$$\mathbf{Q}_{\text{nominal}} = I_i(\mathbf{P}_{\text{nominal}}) \quad (2)$$

The new commanded position $\mathbf{P}_{comp}$ is calculated as in Equation 3 and is then written in a modified G-code. As a reminder, it has been chosen to represent the volumetric error and not to compensate it. This is why $\mathbf{P}_{comp}$ is only the result of the non-ideal forward geometric model. Otherwise, the volumetric error would have been removed to $\mathbf{P}_{\text{nominal}}$ (and not added, as it is here).

$$\mathbf{P}_{comp} = F_{ni}(\mathbf{Q}_{\text{nominal}}) \quad (3)$$

2.3.2. Look-up tables

Another possibility is to fill the linear axis compensation tables of the NC with the imposed geometric errors. Indeed, the machine builder provides a certain number of tables that can be linked to a compensation file for each axis.

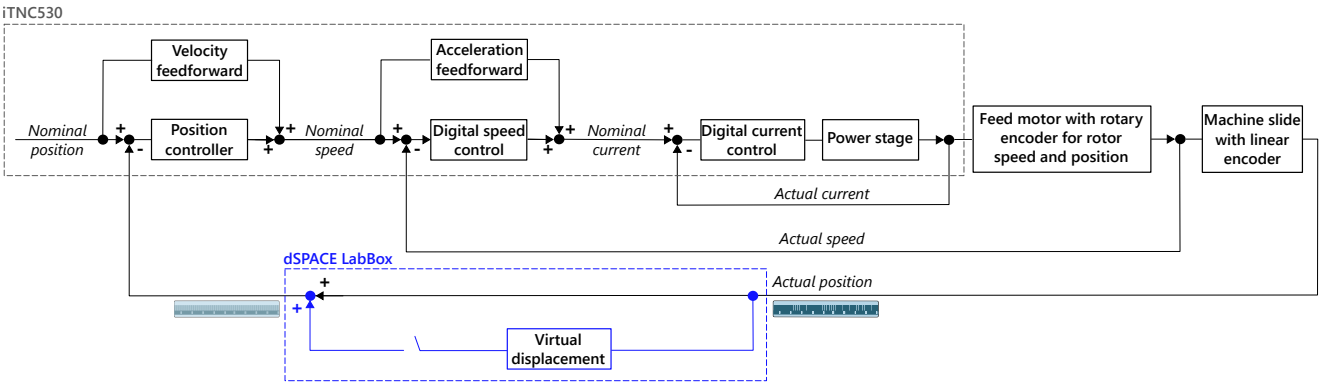

Figure 3: Cascade control loops of the iTNC530, for linear axes, with the addition of a feedback signal modification block. The usual configuration is shown in black (inspired by [26]) [27]

Their input is taken into account by the NC in the position control loop and multi-axis geometric error compensation can occur. These tables are limited in the number of points, therefore the minimum step between to correction points is restricted. This prevents the compensation of sophisticated error functions, such as sudden jerks.

3. Real-time software compensation solution

In this article, the proposed compensation system is the interception and modification of position feedback signals in the machine-tool. The aim is to programmatically assist the NC in generating tool positions that are closer to the desired values, by anticipating the volumetric error deviation in position feedback signals. This software mechanism is outlined in the following section.

3.1. Virtual encoder principle

The linear encoders mounted in the machine-tool used for experiments are Heidenhain DIADUR LS486C. The position information is obtained through the counting of individual increments from any set point of origin. Moreover, an additional track bears distance-coded reference marks. The distance between two marks is unique and provides the absolute reference. This distance is read by the NC during the homing procedure, but also each time the axis crossed these marks during any movement. In the axis control loop of Figure 3, the linear position is estimated once by the motor rotary encoder but the value used in the position control loop is measured by a linear encoder closest to the linear guide-way. In the blue dashed-lined box of Figure 3, the compensation system estimates positions of the axes reading the linear encoder's signals. This information is "instantly" (i.e. at the basic task frequency of 100 kHz) regenerated for the NC. Moreover, a virtual displacement can be gradually added to this position feedback which simulates an axis movement whereas it is not caused by motor rotation. The output of this blue box is the virtual encoder position, and it is the one read by the NC. The position difference between the virtual encoder's data and the actual axis position estimated by the velocity control loop represents a positioning error that the NC compensates by moving its corresponding axes.

The virtual encoder principle [27] is depicted in Figure 4 and can be summarised as follows:

1. In the nominal configuration, the virtual encoder is read by the NC and its value matches the desired joint coordinate X_{nominal}, set by the NC as the nominal position.
2. A gradual displacement is induced on the virtual encoder whereas the actual position X remains the same. The NC compares the commanded position X_{nominal} to the virtual encoder value X_v and measures a positioning error ΔX.
3. The NC signals for a linear displacement to compensate for the previously estimated positioning error. Therefore, the tool is shifted by ΔX in workspace compared to the nominal configuration. The NC assumes that the actual axis position is $X = X_{\text{nominal}}$ while it is $X = X_{\text{nominal}} + \Delta X$.

3.2. Compensation algorithm

In an error compensation application, the virtual displacement magnitude is the result of geometric calculations. However, compared to the strategies exposed in subsection 2.3, the proposed solution is totally independent from the NC and has no link with the machining program. Therefore, because the inputs of the system are the joints coordinates, geometric calculations must be done. The flow chart of Figure 5 can be read as follows :

1. Actual positions (X, Y, Z) of the three axes are estimated through the interpretation of sine and reference tracks of the linear encoders.
2. The volumetric error is estimated in the machine coordinate system (and not in the workpiece coordinate system, from which the program has no information) via the ideal and non-ideal forward geometric models. It is then multiplied by ± 1 whether the user wants to generate or to correct the error in the workspace (this is, once again, very specific to this study, because

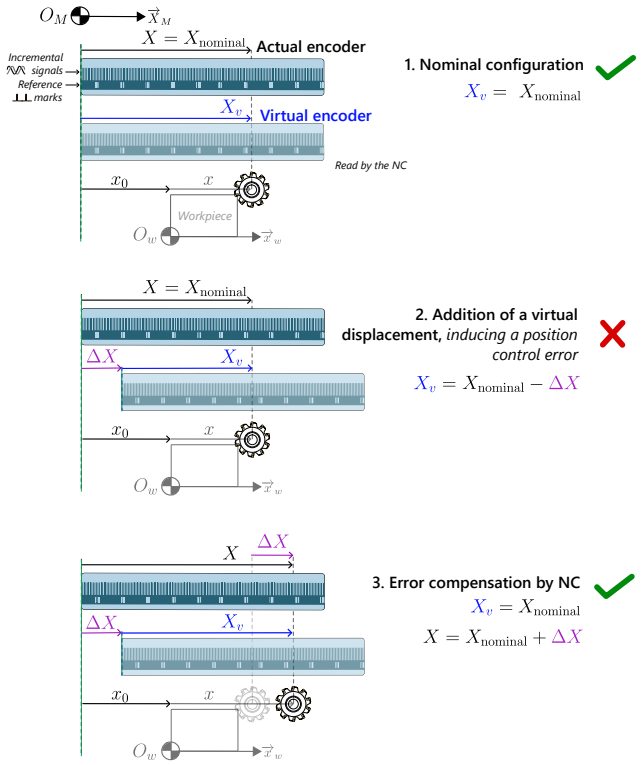

Figure 4: Virtual linear encoder principle: a virtual displacement of the linear encoder induces a real shift of the tool in the workspace (w coordinate system) with no change of the axis position command [27]

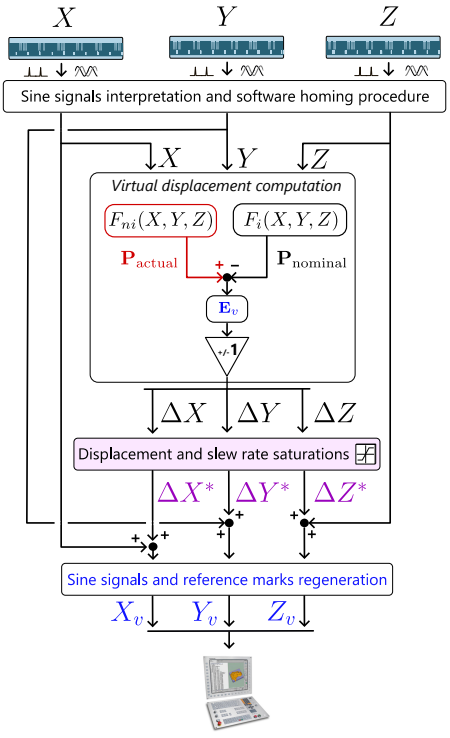

Figure 5: Flowchart of the implemented real-time solution

people usually want to correct the error). Afterwards, as long as no re-orientation of the tool-tip is performed, there is no need to translate the volumetric error from the workpiece to the machine coordinates system, meaning that $\delta x = \Delta X$, $\delta y = \Delta Y$ and $\delta z = \Delta Z$.

3. In case the calculated volumetric error is too big, security blocks saturate the magnitude and rate of change of the virtual displacements sent. This makes the solution safe and robust [27].
4. Error compensation values are added to the copy of the input axis positions, virtual encoders outputs are thus generated.

The real-time software has two different tasks running simultaneously. The basic task, with the highest priority, has a frequency of 100 kHz while the time allowed for the computation of the volumetric error is 6 times longer (17 kHz). The fundamental task ensures the continuity of signals between linear encoders and NC. The signal delay between the encoder's signals acquisition, interpretation, and regeneration is one basic task's period long (i.e. 10 µs). If the axes translate at 10 m min^{-1}, this delay would represent a following error of 1.7 µm. This delay is mostly negligible for the presented purpose, as long as the compensation solution is only used for finishing application during which no machining axis would move that fast.

3.3. Hardware architecture

The proposed real-time compensation software runs on a dSPACE© real-time platform, also called Scalexio LabBox. It is equipped with a DS6001 processor board, DS6121 Multi I/O and DS6221 A/D acquisition boards and the analog signal regeneration is performed by a DS6241 D/A board. These boards have integrated and pre-programmed FPGAs for sine analogue signal reading and generation. The software structure is coded within MATLAB Simulink© and signal conditioning is done with ConfigurationDesk©. Any signal or software's variable can be monitored using the real-time interface running on a computer connected to the LabBox. This allows, for instance, the measurement of the actual encoder's positioning as a function of time.

For more details on the behaviour of the NC to the modification of its position feedback, please refer to [27], in which security blocks implemented to guarantee stability and robustness of the solution are presented.

4. Comparison method of software-based compensation solutions

The performances of the tool positioning correction of this real-time solution were then compared to two other compensation strategies. To do so, the strategies were used as error generation systems instead of error compensation ones, with the main advantage being getting rid of the machine-tool geometric errors estimation's uncertainty.
The results of two compensation experiments are presented

in this article. Motion errors were imposed along the X-axis (section 5) before machining a part that required all 3 linear axes. Hence, this corresponded to a 21-component error model (section 6).

The machining experiments were conducted on a 5-axis machine tool (GFMS HSM600U) with a [w C' B' X b Y Z(C1)t] architecture. The associated NC was a Heidenhain iTNC530 (Figure 3). Only 4 out of 5 axes were needed. Indeed, the machine was used like a 3 linear axis one in the cutting programs, and the rotational movement of the table (C) was only involved to rotate the part, via a workpiece coordinate system reorientation. This allowed the machining of the compared workpieces all to be done in the same area of the machine's workspace. The rotation of the table was not supposed to have any impact on the behaviour of the other axes. Moreover, the compensation tables of linear axes were all disabled, except for the machining of one side of the first presented workpiece, when the performances of these look-up tables were investigated.

The error generation was only involved in the semi-finishing (0.2 mm) and finishing (0.1 mm) operations. Cutting depths were low enough to minimise cutting forces and avoid tool deflection and workpiece distortion. Feature parts were thus roughly prepared a day before. The spindle and axes were warmed-up for at least 10 hours, with a view to avoid thermal expansion of components during machining. For the same purpose, the material of the part was chosen to be a 42CrMo4 steel. The used tool was a carbide solid-end mill, with a 8 mm diameter and 4 teeth (MPMHV from Mitsubishi Materials). It was mounted on a BIG KAISER collet chuck to guarantee a good concentricity (1 µm). The cutting speed was set to 120 m min^{-1}, with a feed per tooth of 0.073 mm.

The performances of the compensation strategies were evaluated using measurements of the axes trajectories before and during the machining. These data were acquired via the real-time proposed software, which was always activated even if no virtual displacements were added to feedback signals (meaning that the compensation part of the program was switched off). Furthermore, workpieces were measured with a high accurate CMM (DEA Global Performance). The test workpieces stayed mounted on the palette for the CMM measurements so as to avoid distortion.

5. Position-dependent geometric errors imposed along X axis

In this first experiment, 3 linear motion errors were simulated along the X axis and the compensation strategies were evaluated in their ability to bring these errors out.

5.1. Geometric errors introduced

As shown in Figure 6, the two error functions chosen have a considerable amplitudes compared to what could naturally be measured along the X-axis. The straightness one is particularly out of the ordinary, and ensures a better identification afterwards.

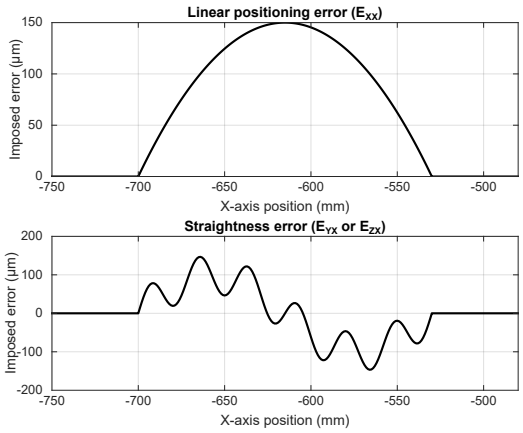

Figure 6: Error functions implemented in the compensation methods

5.2. Workpiece machining strategy

The workpiece geometry (Figure 7) was inspired from the test piece suggested by Pezeshki et al. in [28] for their error identification of a 3-axis machine-tool. The presented part was machined in four steps, because each side correspond with a compensation strategy. For one program (meaning, for one side):

- The slotting of little notches provides proof of the accuracy of positioning along the X-axis (referenced as *a* in Figure 7).
- The flank milling of a vertical plan brings the horizontal straightness error out (referenced as *b* in Figure 7). The Y-axis moves while it is supposed to stay constant in the nominal NC program.
- The end milling of an horizontal plan brings the vertical straightness error out (referenced as *c* in Figure 7). The Z-axis moves while it is supposed to stay constant in the nominal NC program.

As described in Figure 7, the error generation was done differently on each side of the test piece:

1. The first side was machined with the nominal program. This is where machine-tool's defects can be observed, as well as the tool's bending and other machining side-effects. The origin of the workpiece reference frame was set in the center of the square, and the $\vec{z}_w$ axis was supposed to be align with the axis of the rotary table C. A simple change of origin allowed the rotation of the part and the machining of the second side. This machined side serves as the nominal reference, even if it is affected by the unidentified geometric errors of the machine-tool. These geometric errors, along with thermal errors, are considered repeatable within the machine workspace. Therefore

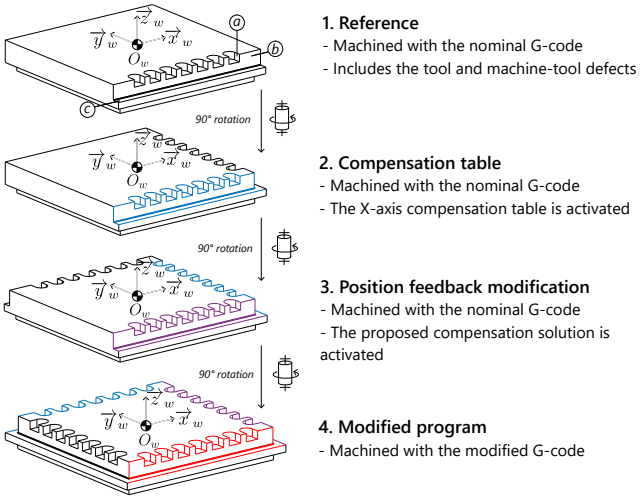

Figure 7: Machining sequence of the test piece

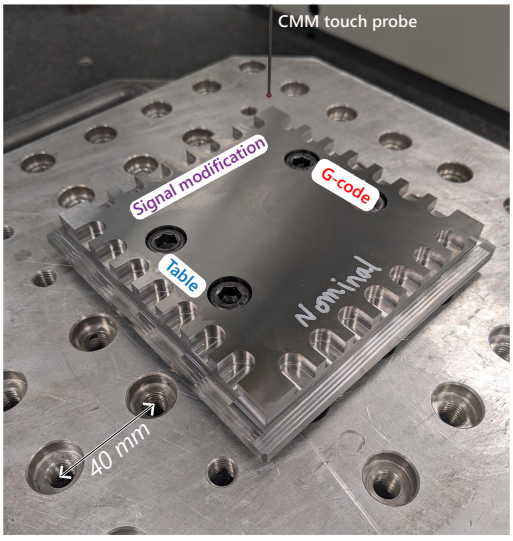

Figure 8: Finished test part during CMM measurement

the four sides of the workpiece are affected in the same way, allowing differential measurement with this side to be performed.

2. For this side, the same program as side n°1 was launched. However, and for this time only, a compensation table filled with the errors depicted in Figure 6 was activated.
3. This side was machined with the same program as sides n°1 and n°2. It is necessary to keep in mind that the interception and regeneration of feedback signals was plugged on during all the machining of the part. Indeed, the joint coordinates **Q** were recorded for strategy comparison purpose. The modification of position feedback was activated for the machining of this side only.
4. The last side was machined with a modified G-code in which the accuracy and straightness errors were artificially introduced.

5.3. Results and discussions

The finished part is displayed in Figure 8.

The planar and notch geometries were measured on a CMM and the results are superimposed in graphs of Figure 9, Figure 10 and Figure 11. The aim of these graphs is to estimate how much the simulated error has been followed along the X-axis. On each figure, the first diagram shows a spatial representation of the Y-, Z- or X-machining trajectory (coloured lines), added to the probed points (coloured error bars, corresponding to $\pm 2\sigma$, σ being the standard deviation) and the imposed error (in black). The second graph displays the difference between the actual trajectory and the commanded geometric error, it can be seen as the following error. In the same graph, the difference between the surface measurement (workpiece geometry) and the commanded geometric error is plotted with error bars. This curve corresponds to the geometric impact of the following error. A last graph is plotted as a zoom, to focus on and compare the performances of the feedback modification solution to the modified G-code method.

For each measured point of the last three sides, the coordinates of the corresponding point of the nominal side were subtracted. The goal of this operation was to remove machining side-effects that would presumably be constant during the machining of the four sides. The CMM measurements were repeated 4 times. Simultaneously, the (X, Y, Z) joint coordinates were measured only once during the machining operations. A back-cutting phenomenon is

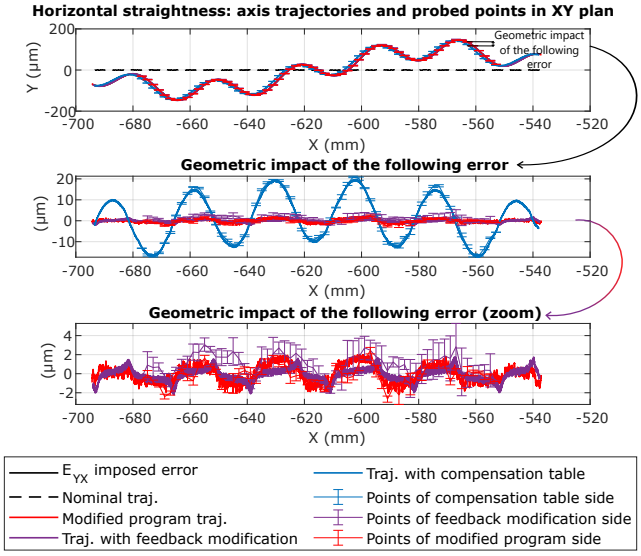

Figure 9: Horizontal straightness results

easily noticeable on the horizontal plan, in the picture of Figure 8 as well as in the probed point cloud of Figure 10. This makes the comparison between Z-axis trajectory and probed points more difficult. Nevertheless, the same trends as in Figure 9 are apparent: a significant following error for

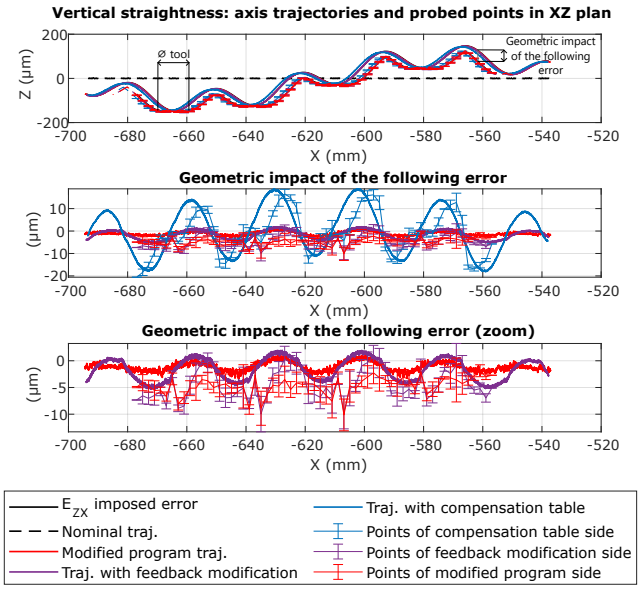

Figure 10: Vertical straightness results

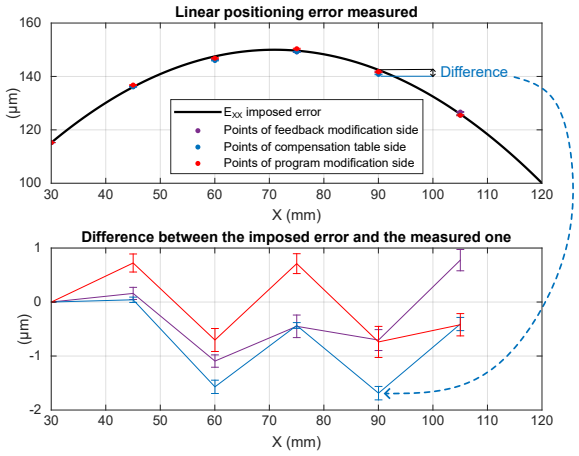

Figure 11: Linear positioning error results

the compensation table and similar performances for the 2 others. The following conclusions can be drawn:

- The use of a modified G-code for error generation performed undeniably well with maximum following error of 2 µm for imposed error ranging from −150 to +150 µm, meaning that more than 98% of the error was generated.
- In the same way, modifying the position feedback provided great results, by bringing out 96% of the imposed error (especially in the Y-direction, graph 9).
- The compensation table results were unsatisfactory. Indeed, the sine blue wave visible in Figure 9 and Figure 10 demonstrates a delay in the compensation consideration, leading to following errors up to 20 µm. No information were found about where the look-up tables are taken into account in the position control loop for the iTNC530 (Figure 3). Further tests were conducted and showed that the response time of the axis compensation is constant, regardless the axis feed-rate. Therefore, it seems that these tables were not considered by the velocity feed-forward block. They are consequently not programmed for sophisticated error function compensation.

Finally, for the positioning of the notches along the X-axis, no difference has been observed between the 3 compensation strategies. Gaps between the imposed error (in black in graph 11) and the actual error (coloured points) are lower that 2 µm, which is close to the CMM measurement uncertainty (1.5 µm). It means that all the compensation methods are equivalent for this type of error. Indeed, the machined plans are perpendicular to the X-axis direction so the Y linear axis had enough time to stabilise itself at the right position during the machining of the notch.

The results of this first experiment show that the proposed solution can perform as well as the program modification while remaining independent from the NC and the program. Furthermore, since the program modification can precisely generate the virtual volumetric error (98%), it is chosen as a solution for virtual volumetric error generation in the following experiment.

6. Position-dependent and -independent geometric errors imposed in a 3-axis machine-tool

The previous experiment allowed the assessment of X-, Y- and Z-axis error correction performances locally. The aim of the second experiment is to simulate a global error compensation scheme, with a 21 geometric errors modelling. The ability of the program modification solution to bring out an error has been highlighted in the previous experiment. Therefore, it is used to create a virtual volumetric error in this section. The compensation table method was set aside, while the two other strategies were used simultaneously. Indeed, three parts were machined: one with a nominal program, one with a modified program, and one with the modified program and the position feedback modification activated so as to machine a piece with the same geometry as the first nominal one.

The geometry of the part was directly inspired from the one referenced as "M1" in the standard ISO 10791-7:2020 [29], designed for assessing the accuracy of a 3-axis machine-tool.

6.1. Geometric errors introduced

The order of magnitude of the chosen errors is lower than those of subsection 5.1. The error functions are order 2 or 3 polynomials [23], as shown in Figure 12. The position-independent errors are given in Table 1. Despite

Table 1
Numerical values of the introduced squareness errors

Position-independent errors	Value ($\mu m\,m^{-1}$)
E_{C0Y}	50
E_{A0Z}	40
E_{B0Z}	20

the small values of the errors along each axis, their impact in the workspace is still significant given that the resultant volumetric error can reach 150 µm.

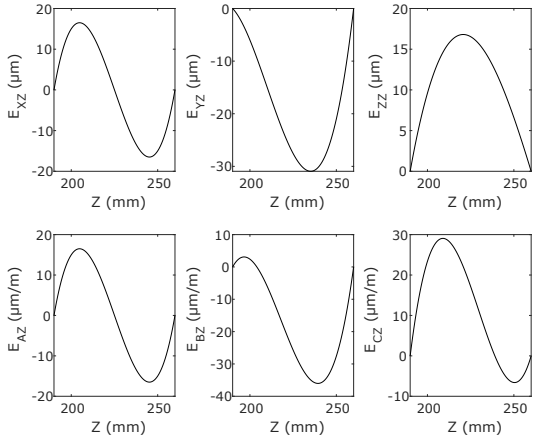

Figure 12: Example of position-dependent errors imposed along the Z-axis

6.2. Results and discussions

The workpieces are presented in Figure 13.

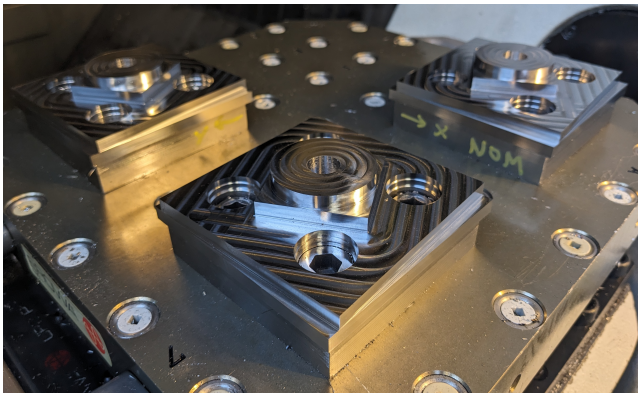

Figure 13: In-situ picture of the machined parts

6.2.1. Tool-path

The joint coordinates measured during machining are compared in Figure 14 and Figure 15. It is obvious that the TCP trajectory was modified by the artificial volumetric error (in red), and that the compensation with position feedback modification (in purple) was effective as long as it is very close to the nominal tool-path (in black). The distance between each point of the compensated and nominal trajectories (error of contour vector) has been evaluated and is plotted for each directions in space in the same figures .

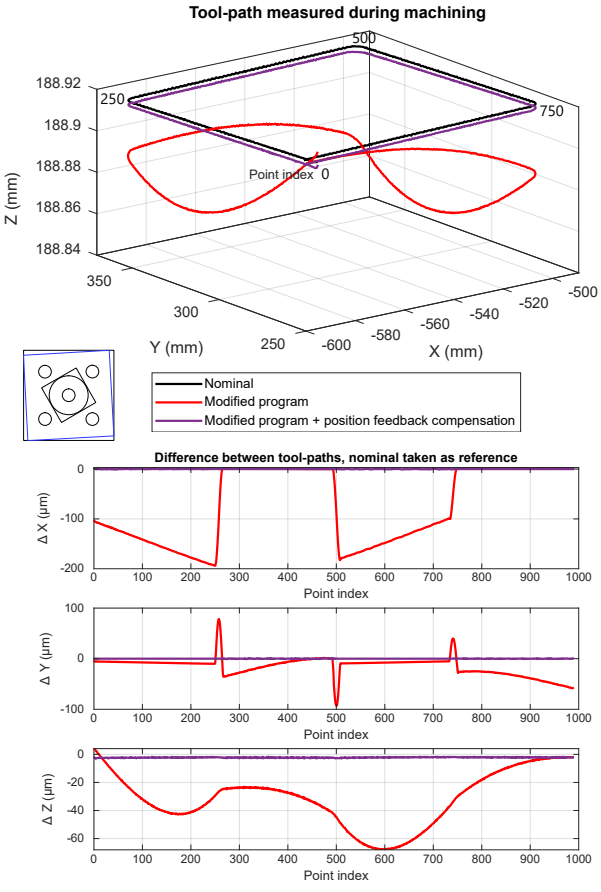

Figure 14: Comparison of some TCP trajectories

Tens of microns have been introduced and compensated for along the 3 axes of the machine. The compensation was 100% effective in the X- and Y-directions because the difference vectors are equal to zero. However, a difference of 5 µm remains in the Z-axis direction between the nominal and the compensated tool-paths. This is only due to machining conditions because the same comparison has been done before cutting and no such observation was made. In Figure 16, the purple dashed curve is coincident with the black dashed circle, meaning that, in air machining conditions, the proposed compensation solution worked perfectly. However, the continuous curves were measured in machining conditions. The vertical shifts measured before and during machining (between the dashed and continuous curves) are different: $\Delta Z_{nom} \neq \Delta Z_{mod} \neq \Delta Z_{comp}$. It means that the machining conditions (cutting forces, tool wear) were not strictly similar between each experiment. For instance, the elasticity of the Z-axis of the used machine is important. For the future, cutting force measurements will be added to ensure a better understanding of the phenomenon.

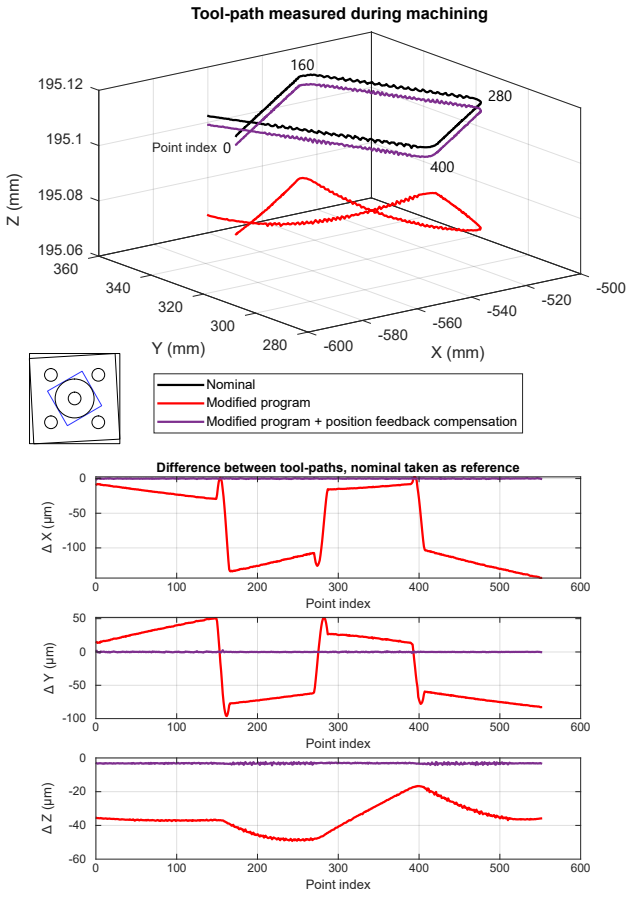

Figure 15: Comparison of some TCP trajectories

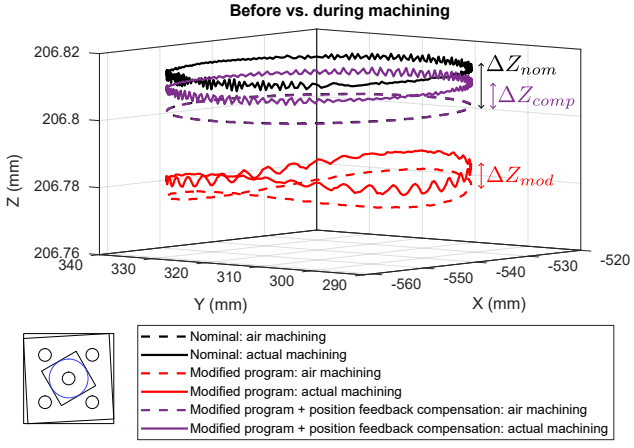

Figure 16: Tool-paths comparison before and during machining

6.2.2. CMM measurements

In the Z-axis direction, the results are analysed through the comparison of the tool-path measurement and CMM probed points in the Figure 17. The least-square plans are plotted in dashed lines. The orientation parameters of these plans are given in Table 2. It is noticeable that the distorted (i.e. modified) red plan has been well corrected to a better oriented (i.e. compensated) one. The differences between the measured flatness are not big enough to draw any conclusions, compared to the rotation angles that are significantly lower for the nominal and compensated plans, in the machine coordinate system.

Table 2
Numerical values of the defects of the measured surfaces and their corresponding least square (LS) plans

	Nominal	Modified	Compensated
Flatness (μm)	2.8	7	5.4
LS plan rotation around $\vec{x}$ (°)	0.0002	0.017	0.0003
LS plan rotation around $\vec{y}$ (°)	0.00017	0.011	0.0003

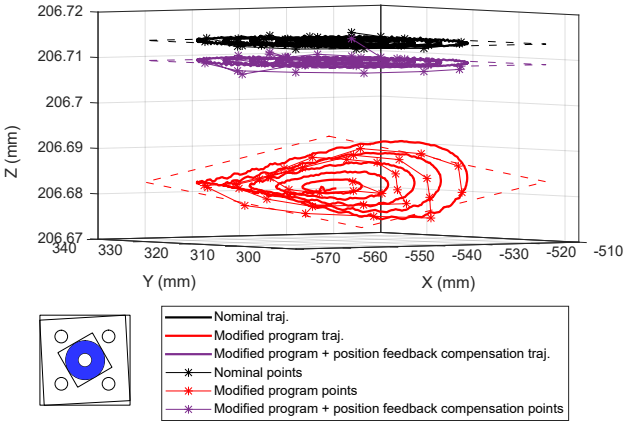

Figure 17: Comparison of the TCP trajectories during the plan end milling and the resulting surfaces and corresponding least square plans

In the following Figure 18 and Figure 19, the point clouds measured with the CMM are compared to a STL file extracted from the CAD model. They were spatially reset via an Iterative Closest Point algorithm (ICP). This allows, for instance, the removal of the translation component of the volumetric error and to look at the geometry distortion of the part only. The measurements were made 6 times each. The standard deviation error bars $\pm\sigma$ are plotted as it is (i.e. with no student factor). They are not all displayed, for readability purposes. Quiver plots of Figure 18 provides information about the geometrical accuracy of the machined part in the XY plan. Figure 19 shows the superposition of the previous plots and allows the assessment of the similarities between the nominal and the compensated workpieces, compared to the one machined with a modified G-code.

The following observations can be made:

- The part machined with the nominal G-code does not perfectly match with the CAD STL file. This could be explained by the defects of the machine, such as a damaged ball screw for the Y-axis for example.

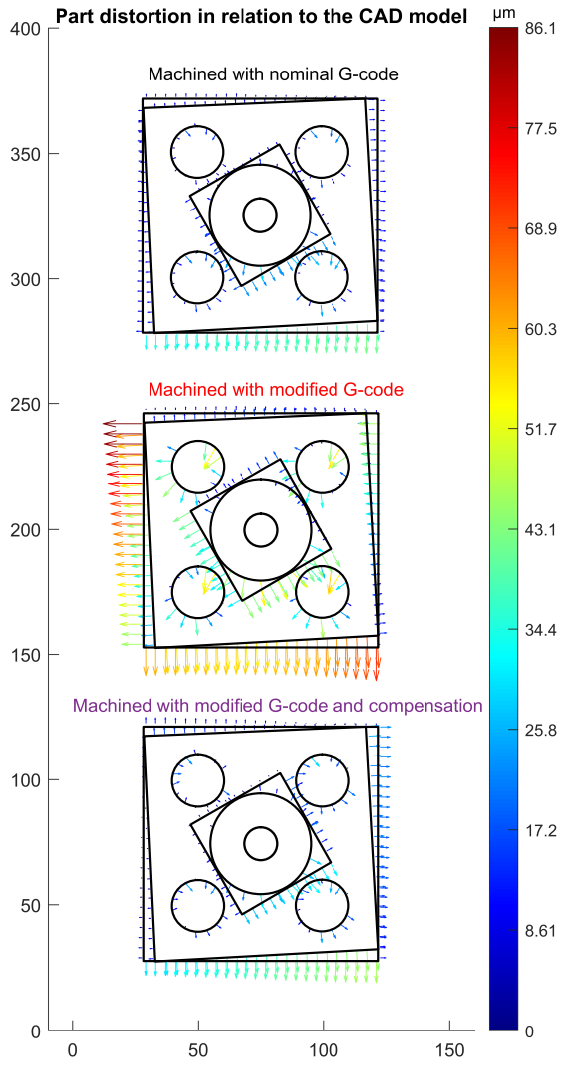

Figure 18: Comparison of the parts geometry in the XY-plan and distortion quantification

- The part machined with the modified program (in the middle of Figures 18 and in red in 19) shows important distortion (up to 86 µm), as expected.
- Figure 19, being the superposition of the items of Figure 18, proves once again that the nominal and the compensated parts are alike (but both still different than the nominal STL). The purple and black lines are well superimposed.

7. Conclusion and perspectives

A geometric error compensation method is presented on the position feedback loop of a CNC machine-tool, in a 3-axis machine-tool. The virtual encoder principle allows small variations of the linear axes position without notifying the NC. With regard to the geometric errors, the position dependent and independent errors of the axes were modelled

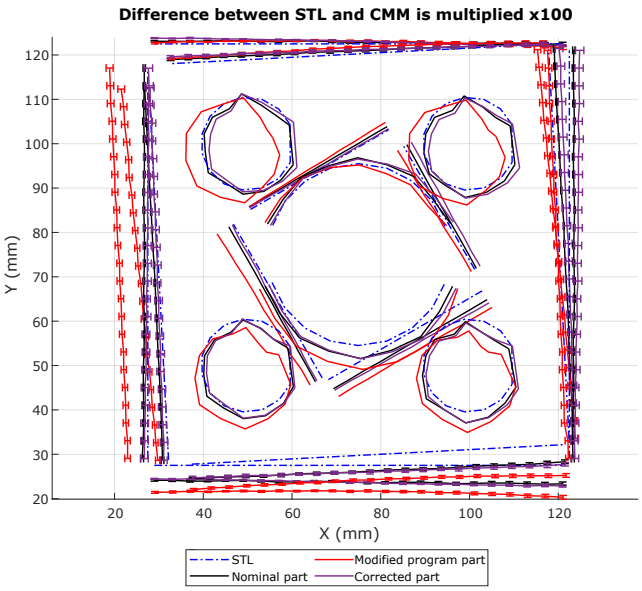

Figure 19: Superposition of the parts geometries in the XY-plan. Differences between STL and CMM are multiplied by 100

and three compensation strategies (NC look-up table, G-code modification, position feedback modification) were tested on their ability to bring out the artificial volumetric error in the first machining experiment. The proposed real-time compensation solution showed promising results. It has been compared to the two other geometric error correction strategies and behaves like the program modification one, by bringing more than 96% of the error out, while remaining independent from the NC and the machining program. It has thus been used like a compensation strategy in a second experiment, in which a virtual volumetric error was added by means of a modified program and imposed geometric error functions. The signal modification solution managed to compensate most of the introduced error, with maximum residuals of 5 µm in the vertical direction, and residuals lower than 1 µm in the XY plane, according to the study of axis trajectories.

The fact that compensation tables are not taken into account in feed-forward control loops makes this conventional solution dependent on axis feed-rate. Therefore, its ability to bring out a virtual volumetric error was lower than the other two compensation strategies in the first machining experiment. For instance, the geometric impact of this following error reached 20 µm. This solution was therefore set aside in the second experiment.

The next step of this research work is the evaluation of the compensation solution's performances in a 5-axis machining application. Moreover, the complexity of the model used for joint compensation calculations could be increased. Indeed, cutting forces or temperature are parameters that change in real-time and could have an impact on the workpiece's final geometry. They could be added as inputs

to the compensation model. For instance, a pre-identified structural deformation model due to thermal effects could be integrated into the proposed solution, along with appropriate temperature measurements. This would enhance the effectiveness of the correction while eliminating the need to generate multiple machining programs based on workshop temperature.

Acknowledgements

This work is part of the CAPTURE5 project , supported by the Cetim (Technical Center for Mechanical Industries) and the french ministry of higher education and research. The dSPACE hardware was provided by ANR JCJC INTEGRATION.

References

[1] W Gao, S Ibaraki, M A Donmez, D Kono, J R R Mayer, Y-L Chen, K Szipka, A Archenti, J-M Linares, and N Suzuki. Machine tool calibration: measurement, modeling, and compensation of machine tool errors. *International Journal of Machine Tools and Manufacture*, 187:104017, 2023. URL https://doi.org/10.1016/j.ijmachtools.2023.104017.

[2] H Schwenke, W Knapp, H Haitjema, A Weckenmann, R Schmitt, and F Delbressine. Geometric error measurement and compensation of machines — an update. *CIRP Annals*, 57:660–675, 2008. URL https://doi.org/10.1016/j.cirp.2008.09.008.

[3] R Ramesh, M A Mannan, and A N Poo. Error compensation in machine tools — a review Part i: geometric, cutting-force induced and fixture- dependent errors. *International Journal of Machine Tools and Manufacture*, 40:1235–1256, 2000. URL https://doi.org/10.1016/S0890-6955(00)00009-2.

[4] L Andolfatto, S Lavernhe, and J R R Mayer. Evaluation of servo, geometric and dynamic error sources on five-axis high-speed machine tool. *International Journal of Machine Tools and Manufacture*, 51: 787–796, 2011. URL https://doi.org/10.1016/j.ijmachtools.2011.07.002.

[5] S Ibaraki and M Hiruya. A novel scheme to measure 2d error motions of linear axes by regulating the direction of a laser interferometer. *Precision Engineering*, 67:152–159, 2021. URL https://doi.org/10.1016/j.precisioneng.2020.09.011.

[6] Y Yao, Y Itabashi, M Tsutsumi, and K Nakamoto. Position error reduction of tool center point in multi-tasking machine tools through compensating influence of geometric deviations identified by ball bar measurements. *Precision Engineering*, 72:745–755, 2021. URL https://doi.org/10.1016/j.precisioneng.2021.08.003.

[7] N Alami Mchichi and J R R Mayer. Axis location errors and error motions calibration for a five-axis machine tool using the samba method. *Procedia CIRP*, 14:305–310, 2014. URL https://doi.org/10.1016/j.procir.2014.03.088.

[8] S Ibaraki, M Sawada, A Matsubara, and T Matsushita. Machining tests to identify kinematic errors on five-axis machine tools. *Precision Engineering*, 34:387–398, 2010. URL https://doi.org/10.1016/j.precisioneng.2009.09.007.

[9] S Sartori and G X Zhang. Geometric error measurement and compensation of machines. *CIRP Annals*, 44:599–609, 1995. URL https://doi.org/10.1016/j.procir.2014.03.088.

[10] M Givi and J R R Mayer. Optimized volumetric error compensation for five-axis machine tools considering relevance and compensability. *CIRP Journal of Manufacturing Science and Technology*, 12:44–55, 2016. URL https://doi.org/10.1016/j.cirpj.2015.09.002.

[11] S Zhu, G Ding, S Qin, J Lei, L Zhuang, and K Yan. Integrated geometric error modeling, identification and compensation of CNC machine tools. *International Journal of Machine Tools and Manufacture*, 52: 24–29, 2012. URL https://doi.org/10.1016/j.ijmachtools.2011.08.011.

[12] RJ Liang, Z Wang, W Chen, and W Ye. Accuracy improvement for RLLLR five-axis machine tools: A posture and position compensation method for geometric errors. *Journal of Manufacturing Processes*, 71:724–733, 2021. ISSN 15266125. URL https://doi.org/10.1016/j.jmapro.2021.09.037.

[13] S M Esmaeili and J R R Mayer. CNC table based compensation of inter-axis and linear axis scale gain errors for a five-axis machine tool from symbolic variational kinematics. *CIRP Annals*, 70:439–442, 2021. URL https://doi.org/10.1016/j.cirp.2021.04.042.

[14] H Lu, Q Cheng, X Zhang, Q Liu, Y Qiao, and Y Zhang. A novel geometric error compensation method for gantry-moving cnc machine regarding dominant errors. *Processes*, 8:906, 2020. URL https://doi.org/10.3390/pr8080906.

[15] Ni J. CNC machine accuracy enhancement through real-time error compensation. *Journal of Manufacturing Science and Engineering*, 119:717–725, 1997. URL https://doi.org/10.1115/1.2836815.

[16] K. T. Navya, V. Shanmugaraj, G. C. Mohan Kumar, and P. V. Shashikumar. A Digital Design Approach and Implementation for Thermal Error Compensation in Machine Tools by Precision Positioning and Feedback Signal Manipulation. *Reason-A Technical Journal*, 12(0):87, July 2013. ISSN 2277-1654. doi: 10.21843/reas/2013/87-92/108142. URL https://informaticsjournals.co.in/index.php/RTJ/article/view/46887.

[17] M. A. Donmez. Progress report of the Quality in Automation project for FY90. Technical report, National Institute of Standards and Technology, 1994.

[18] M. A. Donmez, Yee K. W., and Damazo B. Some guidelines for implementing error compensation on machine tools. Technical report, 1993.

[19] S R Postlethwaite and D G Ford. A practical system for 5-axis volumetric compensation. *Engineering Sciences*, 23:379–388, 1999.

[20] Donatas Gurauskis, Artūras Kilikevičius, and Albinas Kasparaitis. Thermal and Geometric Error Compensation Approach for an Optical Linear Encoder. *Sensors*, 21(2):360, January 2021. ISSN 1424-8220. doi: 10.3390/s21020360. URL https://www.mdpi.com/1424-8220/21/2/360.

[21] Yi Zhou, Weibin Zhu, Yi Shu, Yao Huang, Wei Zou, and Zi Xue. Analysis and application of real-time compensation of positioning precision of the turntable with a harmonic function. *Metrology and Measurement Systems*, pages 553–571, August 2022. ISSN 2300-1941. doi: 10.24425/mms.2022.142269. URL https://journals.pan.pl/dlibra/publication/142269/edition/124549/content.

[22] *Test code for machine tools: Geometric accuracy of machines operating under no-load or quasi-static conditions*. ISO 230-1, 2012.

[23] M. Slamani, J.R.R. Mayer, and G.M. Cloutier. Modeling and experimental validation of machine tool motion errors usinf degree optimized polynomial including motion hysteresis. *Experimental Techniques*, 35(1):37–44, January 2011. ISSN 07328818. doi: 10.1111/j.1747-1567.2009.00576.x. URL http://doi.wiley.com/10.1111/j.1747-1567.2009.00576.x.

[24] Y Abbaszadeh-Mir, J R R Mayer, G Cloutier, and C Fortin. Theory and simulation for the identification of the link geometric errors for a five-axis machine tool using a telescoping magnetic ball-bar. *International Journal of Production Research*, 40(18):4781–4797, January 2002. URL https://doi.org/10.1080/00207540210164459.

[25] S Ding, Z Song, Z Chen, We Wu, and A Song. An efficient geometric error modelling algorithm of CNC machine tool without interference of higher-order error terms. *The International Journal of Advanced Manufacturing Technology*, 126(7-8):3353–3366, 2023. URL https://doi.org/10.1007/s00170-023-11297-1.

[26] *Technical manual iTNC530*. Heindehain, 2006.

[27] F Guevel, C Euzenat, F Viprey, and G Fromentin. Response of a numerically-controlled machine-tool to the modification of its position feedback using real-time solution. In *Proceedings of the 24th International Conference of the European Society for Precision Engineering and Nanotechnology*. euspen, 2024.

[28] M Pezeshki and B Arezoo. Kinematic errors identification of three-axis machine tools based on machined work pieces. *Precision Engineering*, 43:493–504, 2016. URL https://doi.org/10.1016/j.precisioneng.2015.09.018.

[29] *Test conditions for machining centres: Accuracy of finished test pieces*. ISO 10791-7, 2020.